Engineering Structures 33 (2011) 2919–2930

Contents lists available at ScienceDirect

Engineering Structures

journal homepage: www.elsevier.com/locate/engstruct

# A probabilistic boundary element method applied to the pile dislocation problem

Samer Sabry F. Mehanny [a], Sameh S.F. Mehanny [a,b,*], Youssef F. Rashed [b,c]

[a] Department of Bridges & Special Structures, Dar Al-Handasah, Mohandessin, Giza, Egypt

[b] Department of Structural Engineering, Cairo University, Egypt

[c] Department of Civil Engineering, British University in Egypt, Egypt

ARTICLE INFO

*Article history:*
Received 10 June 2010
Received in revised form
12 June 2011
Accepted 14 June 2011
Available online 16 July 2011

*Keywords:*
Boundary elements
Pile
Dislocation
Codes
Monte Carlo simulation

ABSTRACT

In this paper a probabilistic approach is presented where the boundary element method is efficiently used to study the effect of a random shift of a given pile within a particular pile cap from its original position – the so-called *pile dislocation* problem – on selected output design parameters such as pile loads and bending moments in the pile cap. A new circular internal element is developed to simulate the true geometric modeling of piles. The boundary element method for the shear-deformable (thick) plate theory is employed to analyze the pile cap. The plate–pile interaction forces are considered to have constant variation over the circular pile domain. The probabilistic approach presented herein incorporates a Monte Carlo simulation technique for generating random shifts in the original position of a given pre-selected pile. The procedure has been applied to some exemplar pile caps with given pile layouts typically adopted in bridge construction.

The results demonstrate that the random dislocation of piles within practical ranges/values as customarily encountered for example in pile caps pertinent to bridge applications will cause limited variations in the output design parameters investigated herein and mentioned above. In other words, it has been illustrated that the resulting dispersion in the output values due to random dislocation of piles is less than the possible intrinsic dispersion that may be practically triggered in the pile locations due to common construction inaccuracies and/or unanticipated problems during pile driving process. The study further emphasizes the efficiency and reliability of the Boundary Elements Method adopted herein for such application.



## 1. Introduction

Effects of pile dislocation on the safety of bridges' pile caps under a bi-axial loading state are of utmost importance to the bridge design community. Pile dislocation is occasionally occurring due to frequent and highly likely construction inaccuracies expected on site for this somehow large civil structures. Such inaccuracies are not uncommon due to often harsh construction conditions usually encountered on site for large bridges crossing profound valleys or deep waters. The current paper is a step forward aiming at studying the pile dislocation effects on some selected design parameters/straining actions including the pile load and bending moments in the pile cap, and hence demonstrating whether such effects are of much importance to the overall safety of the as-designed structure or not. The present work is conducted in the context of a probabilistic investigation using the Boundary Elements Method (BEM) to model both piles and pile cap, along with Monte Carlo (MC) simulation techniques to mimic possible random dislocation (geometric shift) of a particular pile within a given pile cap featuring a certain configuration of piles. MC techniques have been extensively and effectively used in the literature to model randomness and uncertainties in a variety of civil and structural engineering applications (e.g., [1–4]).

The efficiency and reliability of the BEM in such application is due to the fact that each time the pile is randomly assumed to be slightly shifted from its original location, a complete re-meshing of the whole domain depicting the case-study problem is not required. Conversely, a sophisticated re-meshing is generally a must for the re-analysis of such dislocation situations with other conventional and well-established methods of analysis such as the Finite Element Method (FEM). Moreover, even with the availability of advanced software providing automatic mesh/re-mesh generation techniques for FEM analysis, the outcome of the analysis is not able to isolate the effect of the randomness in pile dislocation on the variability in the piles/pile cap response from the effect of the intrinsic uncertainty (namely, the *epistemic* modeling uncertainty) coming from the variability and randomness in the different meshes resulting from the adopted re-meshing technique.

* Corresponding author at: Structural Engineering Department, Cairo University, Egypt. Tel.: +20 12 444 8008.
*E-mail address:* sameh.mehanny@stanfordalumni.org (S.S.F. Mehanny).

0141-0296/$ – see front matter © 2011 Elsevier Ltd. All rights reserved.
doi:10.1016/j.engstruct.2011.06.016

The literature has not been generous in discussing and tackling the pile dislocation problem although the consequences of such accidental events may be detrimental in a number of cases. From the limited information available in the literature concerning this issue, it is well conceived that pile construction specifications commonly allow about 3 inches (75 mm) of "accidental" pile dislocation from the original (i.e., design) location [5]. A pile dislocation generally shifts the center of gravity of the group of piles resulting in an eccentric loading condition even if the original load is concentric with respect to the group of piles. This incident increases the load on some piles and reduces the load on others. Small groups of say two to four piles are most susceptible to overload. For example, a 4-pile cluster spaced at 3 ft (about 900 mm) center to center subjected to the loosely speaking "optimum" dislocation of up to 3 inches (75 mm) mentioned above causes the most heavily loaded pile to be overloaded to 124% of its average load [5]. This effect diminishes as the number of piles in the group increases. AASHTO specifications [6] therefore wisely suggest that such dislocation be considered in design especially for small groups of piles. Moreover, the maximum compressive load on any pier or pile due to dislocation shall not be more than 110% of the allowable design load as spelled out in [7]. On the same issue of pile dislocation, it has been customarily demonstrated that the preferred minimum group of piles for a concentrated load has to be formed of three piles, typically arranged in a symmetrical triangular pattern with piles spread a minimum distance usually at least 30–60 inches (760–1520 mm) center to center, and that for such arrangement a small dislocation of the column's and/or pile group's centroid is usually tolerated [8]. Generally speaking, if one of the piles is slightly dislocated during the pile driving process, it may be possible to alter the location of the rest of the group to compensate for such shift. However, if the dislocation cannot be adjusted (i.e., back-accounted for) in this re-arrangement manner, it becomes necessary to add more piles to the group in order to regain a reasonable alignment of the column and the group's centroid. Re-arranging the piles or adding extra piles to accommodate pile dislocation problems is nonetheless not practically always possible; and hence studying the effect of such dislocation on the original configuration is of a significant importance to the design community. In the present paper, the pile dislocation issue applied to generic case-study problems with moderate number of piles and given typical arrangement of piles will be investigated through a probabilistic framework as illustrated in the sequel, and its effect will be then quantified through commonly applied statistical measures.

In the current research, piles are considered with their real circular geometry. A special and new BEM formulation has been developed and implemented for that purpose which improves the geometric modeling of the problem and consequently enhances the accuracy of the results. The present work plan starts by selecting a base case-study pile cap with a given configuration of piles. A smart BE mesh is then generated to model the problem geometry and loadings using a specialized software [PLPAK] developed by the authors [9,10]. A Monte Carlo simulation is then performed through randomly generating a large number of values describing different dislocations of a given pile within the pile cap according to appropriately assumed Probability Distribution Functions (PDF). This step is done using the Matlab Ver. 6.0 [11] computational platform. Several piles within the given selected configuration (i.e., corner, edge and central piles, if applicable) could be assumed to be individually randomly dislocated for the purpose of the current study. The BE model is run thousands of time for randomly generated dislocations and results are reported. Post-processing for the results of such statistical Monte Carlo-BEM analysis simulations – with overwhelming amount of output – is definitely a challenge and has therefore been automated in the current research. Several statistical measures have been computed for the randomly generated results including averages of piles load and bending moments in the cap, as well as estimates for the dispersion in these quantities using standard deviations, COV, and percentiles. Evaluation of retrieved estimates for variations (i.e., dispersions) in the values of the above mentioned design parameters provides a keystone for an inclusive and robust performance-based design framework aiming at assessing the safety of pile caps enduring pile dislocation problems.

To conclude, it is worth highlighting the fact that the contribution of the present study is intended to be along two lines: (1) provide to the research community a special Boundary Element formulation of a new circular element capable of *efficiently* and *accurately* modeling the pile with its *actual circular* geometry which enhances the accuracy of the analysis results; and (2) study the practical problem of the pile dislocation and its implication to the foundation design practice for some representative and commonly encountered "pile cap–pile" configurations especially in bridge construction. It should be also noted that foundation design codes address effect of pile dislocation only on pile loads and disregard its effect on the other equally important design parameter which is the bending moment in the pile cap. Therefore, the investigation conducted in the current research to study the effect of pile dislocation on the variation in design bending moments in the pile cap constitutes another important contribution to the foundation design practice.

## 2. Boundary elements applied to pile caps

Consider an arbitrary pile cap with domain $\Omega$ and boundary $\Gamma$, loaded by domain loading $q$ and series of column patch areas $c$. The indicial notation is used in this section where the Greek indexes (namely, $\alpha$ and $\beta$) vary from 1 to 2 (to denote the $x$ and $y$ directions) and Roman indexes (namely, $i, j$ and $k$) vary from 1 to 3 (to denote the $x, y$ and the $z$ directions). The Reissner plate bending theory [12] is used herein to account for the shear deformation result from the cap thickness. The cap is a traction free plate supported over series of piles $p$. It is assumed that piles are connected to the cap over circular patches. Three interaction forces are considered: two bending moments in the two directions and one vertical shear. The direct boundary integral equation for such a cap can be written in the light of the formulations presented by Rashed [9,10]:

$$\begin{aligned}
&C_{ij}(\xi)u_j(\xi) + \int_{\Gamma(x)} T_{ij}(\xi,x)u_j(x)\,\mathrm{d}\Gamma(x) \\
&\quad = \int_{\Gamma(x)} \left[V_{i,n}(\xi,x) - \frac{\nu}{(1-\nu)\lambda^2}U_{i\alpha}(\xi,x)\right] q\,\mathrm{d}\Gamma(x) \\
&\qquad + \sum_c \left\{ \int_{\Omega c(y)} \left[U_{ik}(\xi,y) - \frac{\nu}{(1-\nu)\lambda^2}U_{i\alpha,\alpha}(\xi,y)\delta_{3k}\right] \right. \\
&\qquad \left. \times\,\mathrm{d}\Omega_c(y) \vphantom{\int} \right\} F_k(y) \\
&\qquad + \sum_p \left\{ \int_{\Omega p(y)} \left[U_{ik}(\xi,P) - \frac{\nu}{(1-\nu)\lambda^2}U_{i\alpha,\alpha}(\xi,P)\delta_{3k}\right] \right. \\
&\qquad \left. \times\,\mathrm{d}\Omega_p(P) \vphantom{\int} \right\} \times \left[\frac{-u_k(P)S_k(P)}{A(P)}\right] \qquad (1)
\end{aligned}$$

where, $T_{ij}(\xi,x)$, $U_{ij}(\xi,x)$ are the two-point fundamental solution kernels for tractions and displacements respectively [13]. The two points $\xi$ and $x$ are the source and the field points respectively. $u_j(x)$ and $t_j(x)$ denote the boundary generalized displacements and tractions. $C_{ij}(\xi)$ is the jump term and the kernel $V_i(\xi, x)$ is a suitable particular solution to represent domain loading [13]. $A(P)$ is the area of the circular pile cross-section with a center $P$, $F$ is the pile force, i.e., load, and $u_k$ is the boundary generalized displacement in the $k$ direction. $\delta$ refers to the identity matrix. The symbols $\nu$ and $\lambda$ denote the plate Poison's ratio and shear factor. The symbol $c$ denotes the number of internal column patches (applied loading elements) with domains $\Omega_c$ whereas the symbol $p$ denotes the number of internal supporting piles with domains $\Omega_p$. The field points $y$ and $P$ denotes the point of the internal column or pile center, respectively. $S_k$ represents the bending and the axial stiffness of the column. It has to be noted that no summation is considered over the $k$ index in all equations in this section.

Eq. (1) represents three integral equations. Such equations can be written at each boundary node $\xi$ and also at each column center to form a system of linear equations. Boundary values $u_j(x)$ together with generalized displacements at internal pile centers can be obtained from the solution of such system of equations. Integrals over the circular pile domains will be presented in the next section.

Internal values at any internal point $\xi$ can be computed as post-processing stage. For example, displacements at internal points can be computed using Eq. (1) using $C_{ij}(\xi) = \delta_{ij}$ (the identity matrix). Whereas straining action values (bending moments $M_{\alpha\beta}$ and shear forces $Q_{3\beta}$) can be computed using other integral equations as follows [9,10]:

$$\begin{aligned} M_{\alpha\beta}(\xi) &= -\int_{\Gamma(x)} T_{\alpha\beta k}(\xi, x) u_k(x) \mathrm{d}\Gamma(x) \\ &+ q\int_{\Gamma(x)} W_{\alpha\beta}(\xi, x)\mathrm{d}\Gamma(x) + \frac{\nu}{(1-\nu)\lambda^2} q\delta_{\alpha\beta} \\ &+ \sum_c \left\{ \int_{\Omega_c(y)} \left[ U_{\alpha\beta k}(\xi, y) - \frac{\nu}{(1-\nu)\lambda^2} U_{\alpha\beta\theta,\theta}(\xi, y)\delta_{3k} \right] \right. \\ &\left. \times\, \mathrm{d}\Omega_c(y) \right\} F_\alpha(y) \\ &+ \sum_P \left\{ \int_{\Omega_P(y)} \left[ U_{\alpha\beta k}(\xi, P) - \frac{\nu}{(1-\nu)\lambda^2} U_{\alpha\beta\theta,\theta}(\xi, P)\delta_{3k} \right] \right. \\ &\left. \times\, \mathrm{d}\Omega_p(P) \right\} \times \left[ \frac{-u_k(P) S_k(P)}{A(P)} \right] \end{aligned} \tag{2}$$

and

$$\begin{aligned} Q_{3\beta}(\xi) &= -\int_{\Gamma(x)} T_{3\beta k}(\xi, x) u_k(x)\mathrm{d}\Gamma(x) + q\int_{\Gamma(x)} W_{3\beta}(\xi, x)\mathrm{d}\Gamma(x) \\ &+ \sum_c \left\{ \int_{\Omega_c(y)} \left[ U_{3\beta k}(\xi, y) - \frac{\nu}{(1-\nu)\lambda^2} U_{3\beta\theta,\theta}(\xi, y)\delta_{3k} \right] \right. \\ &\left. \times\, \mathrm{d}\Omega_c(y) \right\} F_3(y) \\ &+ \sum_P \left\{ \int_{\Omega_P(y)} \left[ U_{3\beta k}(\xi, P) - \frac{\nu}{(1-\nu)\lambda^2} U_{3\beta\theta,\theta}(\xi, P)\delta_{3k} \right] \right. \\ &\left. \times\, \mathrm{d}\Omega_P(P) \right\} \times \left[ \frac{-u_k(P) S_k(P)}{A(P)} \right]. \end{aligned} \tag{3}$$

The relevant new kernel $U_{ijk}$, $T_{ijk}$ and $W_{i\beta}$ and their relevant derivatives are given in Refs. [9,10,12]. It has to be noted that all kernels at internal points are smooth, and could be straightforwardly computed even over pile centers.

Eqs. (1)–(3) are implemented by the authors into the software package PLPAK as part of the current research.

## 3. Circular pile element

In this work, a new BEM element is introduced and implemented to model piles with their real circular geometry. In order to compute integrals over the pile domains $\Omega_p$ in Eqs. (1)–(3), the technique is presented. The coordinates of any internal point P inside a pile could be expressed in the following polar coordinates:

$$x_1(P) = r(P)\cos\theta(P) \tag{4}$$

$$x_2(P) = r(P)\sin\theta(P). \tag{5}$$

If the natural variable $\varsigma$ (ranges from $-1$ to $+1$) is used to transform $r(P)$ (which ranges from 0 to $R$; in which $R$ is the pile radius), this gives:

$$r(P) = (\zeta + 1)\frac{R}{2}. \tag{6}$$

Similarly, the natural variable $\eta$ (ranges from $-1$ to $+1$) is used to transform $\theta(P)$ (which ranges from 0 to $2\pi$), this gives:

$$\theta(P) = (\eta + 1)\pi. \tag{7}$$

Substitute from (6) and (7) into (4) and (5), to give

$$x_1(P) = (\zeta + 1)\frac{R}{2}\cos[(\eta + 1)\pi] \tag{8}$$

$$x_2(P) = (\zeta + 1)\frac{R}{2}\sin[(\eta + 1)\pi]. \tag{9}$$

Hence the integral of any function $(\bullet)$ over the circular domain $\Omega_P$ can be expressed as follows:

$$\int_{\Omega_p} (\bullet)\mathrm{d}\Omega(P) = \int_{x_1}\int_{x_2} (\bullet)\mathrm{d}x_2\mathrm{d}x_1 = \int_{-1}^{+1}\int_{-1}^{+1} (\bullet)|\mathbf{J}|\mathrm{d}\zeta\mathrm{d}\eta. \tag{10}$$

Where $|\mathbf{J}|$ is the Jacobian of transformation and given by [14]:

$$|\mathbf{J}| = \begin{vmatrix} \dfrac{\partial x_1}{\partial \zeta} & \dfrac{\partial x_1}{\partial \eta} \\ \dfrac{\partial x_2}{\partial \zeta} & \dfrac{\partial x_2}{\partial \eta} \end{vmatrix}. \tag{11}$$

Consider Eqs. (8) and (9), the following derivatives can be obtained:

$$\frac{\partial x_1}{\partial \zeta} = \frac{R}{2}\cos[(\eta + 1)\pi] \tag{12}$$

$$\frac{\partial x_1}{\partial \eta} = -\pi(\zeta + 1)\frac{R}{2}\sin[(\eta + 1)\pi] \tag{13}$$

$$\frac{\partial x_2}{\partial \zeta} = \frac{R}{2}\sin[(\eta + 1)\pi] \tag{14}$$

$$\frac{\partial x_2}{\partial \eta} = \pi(\zeta + 1)\frac{R}{2}\cos[(\eta + 1)\pi]. \tag{15}$$

Substitute of the former derivatives in Eqs. (12)–(15) into Eq. (11) to give:

$$|\mathbf{J}| = \left| \frac{\pi R^2}{4}(\zeta + 1) \right|. \tag{16}$$

It is easy to carry out simple check to verify the former formulation, as follows:

If (•) is considered to be unit, the value of the integral should be equal to the area of the domain cell $C$:

$$\text{Area} = \int_{\Omega} 1 \mathrm{d}\Omega = \int_{-1}^{+1}\int_{-1}^{+1} 1|\mathbf{J}|\mathrm{d}\zeta\,\mathrm{d}\eta$$
$$= \int_{-1}^{+1}\int_{-1}^{+1} \frac{\pi R^2}{4}(\zeta+1)\mathrm{d}\zeta\,\mathrm{d}\eta = \pi R^2 \qquad (17)$$

which verifies the former formulation. It has to be noted that integrals over the piles and circular columns (if any) in Eqs. (1)–(3) are carried out using the formulation presented in this section.

The new formulation presented in this section is as well implemented by the authors in PLPAK software package as part of the current research.

## 4. Case-study problems, BEM verification works and details of the probabilistic approach

The probabilistic BEM investigated herein has been first applied to a generic case-study base problem depicting a regular pile cap that is rectangular in plan and supported on a matrix of six piles (refer to Fig. 1). The pile cap dimensions in plan are 9.6 × 7.0 m. The pile diameter has been picked as 1.2 m, and the pile configuration is selected as three piles in the long direction of the pile cap (namely, the $x$-direction) with equal spacing of three times the pile diameter, and two piles in the short direction (namely, the $y$-direction) with a spacing of 4.6 m. A typical pile cap depth of 1.6 m has been considered. This overall thickness has been varied for a few investigated cases in the course of the parametric study performed in the present research in order to explore its effect on the resulting design quantities and their dispersion. A column is located at the centroid of the pile cap's rectangular footprint. The column has a rectangular cross-section with a 1.5 m width along the short direction of the pile cap and 5.5 m length along the longitudinal direction. The axial stiffness of each of the six piles supporting the cap in the BEM model has been chosen as $2200 \times 10^3$ kN/m representing an actual realistic value of bearing stiffness for piles resting on good soil/rock.

Two additional problems (refer to Fig. 2) with smaller number of piles as commonly encountered in practice in typical bridge construction are also investigated: a triangular pile cap with a 3-pile configuration, and a square pile cap with a 4-pile configuration. These two problems along with the case-study base problem representing a rectangular pile cap with a 6-pile configuration introduced above expand the practical side of the study and hence broaden the conclusions to be drawn from the present investigation. All geometric features of the two additional problems are depicted in Fig. 2.

For the parametric numerical study conducted herein, the case of a bi-axially loaded pile cap has been considered. Two sets of bi-axial column's stress resultants typical to seismic load combinations, referred to by (1) "ordinary" moments condition, and (2) "increased" moments condition, have been investigated. The first set represents short to medium height piers, while the second represents fairly long piers. The pile cap own weight has been considered in addition to the loading values transferred through the column. The ratios of the applied bending moments around the two principal axes of the column to the applied normal force have been taken as $M_x/N = 3.0$ m and $M_y/N = 1.0$ m, and $M_x/N = 5.5$ m and $M_y/N = 2.0$ m for the *ordinary* and *increased* moments conditions, respectively. The assumed geometric and loading characteristics of the case-study problems are representative of typical actual situations encountered in the bridge design practice.

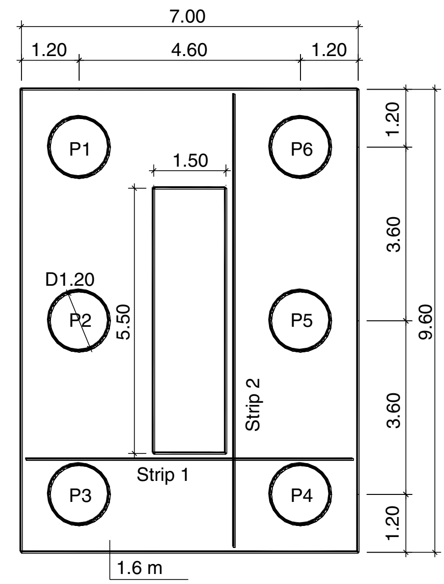


**Fig. 1.** Main geometric characteristics of the case-study base problem including pile naming system and location of reported bending moment results.

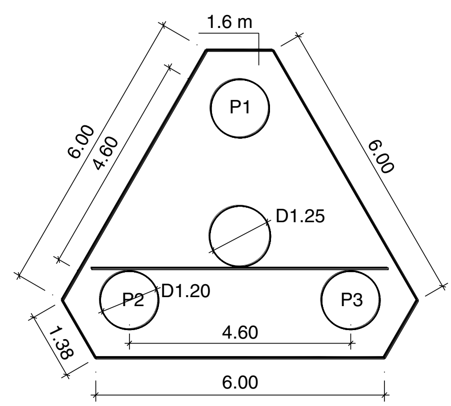


**Fig. 2a.** Main geometric characteristics of the 3-pile configuration case-study problem including pile naming system and location of reported bending moment results.

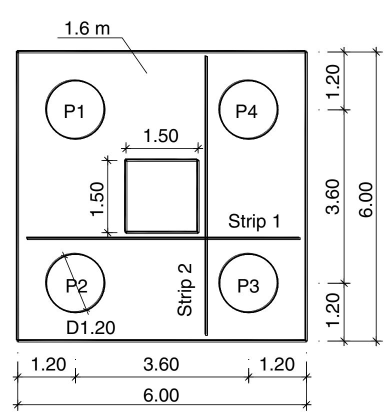


**Fig. 2b.** Main geometric characteristics of the 4-pile configuration case-study problem including pile naming system and location of reported bending moment results.

### 4.1. BEM verification/validation example

Before proceeding with the probabilistic BEM study, it was found prudent to present a numerical verification/validation of the deterministic BEM model (along with the new formulation of

**Table 1**
Pile loads of the case-study base problem (6-pile configuration) under ordinary moments condition retrieved from BEM (PLPAK software) and FEM (Sap 2000 software) analyses.

| Pile no. | BEM (PLPAK) | FEM (Sap 2000) Mesh (shell element) size 0.4 × 0.4 m | | FEM (Sap 2000) Mesh (shell element) size 0.2 × 0.2 m | |
|---|---|---|---|---|---|
| | Pile load (kN) | Pile load (kN) | $P_{BEM}/P_{FEM}$ | Pile load (kN) | $P_{BEM}/P_{FEM}$ |
| P1 | −844 | −833 | 1.01 | −849 | 0.99 |
| P2 | 1690 | 1670 | 1.01 | 1702 | 0.99 |
| P3 | 3323 | 3333 | 1.00 | 3317 | 1.00 |
| P4 | 4690 | 4699 | 1.00 | 4680 | 1.00 |
| P5 | 3305 | 3286 | 1.01 | 3325 | 0.99 |
| P6 | 523 | 533 | 0.98 | 513 | 1.02 |

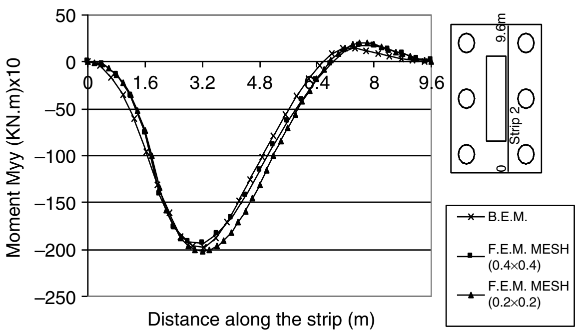


**Fig. 3.** $M_{yy}$ along strip 2 for the base problem under "ordinary" moments condition—BEM versus FEM deterministic results.

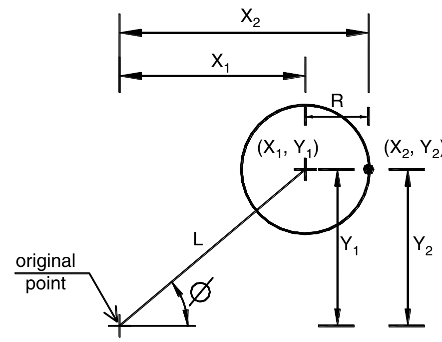


**Fig. 4.** Schematic for the random shift of pile location.

the circular element presented herein) and the results generated using PLPAK software for the case-study base problem of the 6-pile configuration. Generated BEM results using PLPAK software are compared to FEM results using SAP 2000 [15] software. Comparisons are given in a tabular format (Table 1) for pile loads and in a graphical format (Fig. 3) for the bending moments in the pile cap. The bending moment, $M_{yy}$, along a strip located at the face of the column and near the side of the most stressed pile in compression, P4, and parallel to the pier longest direction (see Fig. 3) is selected as an example of internal forces and is shown for comparison purposes. Two FEM mesh sizes for the pile cap (namely, using 0.2 × 0.2 m and 0.4 × 0.4 m shell elements, respectively) have been tried for mesh sensitivity analysis purposes and for completeness. Results shown in Table 1 and Fig. 3 are both for the "ordinary" moments condition stated above. For additional and detailed results of the verification study, the reader may refer to [16]. Presented comparative results show very good agreement between the output of both BEM and FEM analyses.

### *4.2. Details of the probabilistic approach*

A Monte Carlo simulation is then performed by randomly generating a large number of shifts (i.e., dislocation) in the center of a particular pile out of the six piles within the base case-study pile cap according to appropriate Probability Distribution Functions (PDF). This random generation step is done using the Matlab Ver. 6.0 [11] computational platform. Several piles within the given selected configuration (i.e., different corner and edge piles) are assumed to be *individually* randomly dislocated for the purpose of the current study. Only the results of a randomly dislocated *corner* pile are presented in the current paper for space limitations. This corner pile has been selected as the most stressed one taking into account the particular orientations of the applied moments assigned to the case-study base problem. Three types of generated random pile dislocation have been also considered, namely: a random *x*-direction-only movement, a random *y*-direction-only movement, and a random general movement. The results of only the latter – more general and practically frequent – case are presented in this paper. For further detailed results corresponding to randomly dislocating other piles with various types of dislocation the reader may refer to [16]. Note that dislocation of only one pile at a time is considered as mentioned above; i.e., possible concurrent dislocations of different piles within the pile cap and corresponding correlations between such simultaneous dislocations are ignored at present. This situation is however currently under scrutiny by the authors. In order to generate a set of thousands of random dislocated positions of a (*single*) particular pile – independently from other piles – according to an adopted PDF, two random variables are *separately* generated. The first random variable is the angle Øbetween the generally inclined line joining the original (i.e., before dislocation) center of the dislocated pile and its center after dislocation, and a horizontal line passing through this original center. The second random variable is the length $L$ of this line joining the original center and the shifted center of the dislocated pile (refer to Fig. 4). It is worth noting that a *uniform* PDF has been intuitively used to generate random values of Ø, while a *truncated normal* PDF has been considered in generating random values of $L$. The "*truncated*" normal PDF is deemed necessary while dealing with the random variable $L$ in order to avoid having the dislocated pile falling outside the pile cap layout as a result of the random generation which is practically not possible. It is worth stating that the results presented in the sequel (either in terms of pile reaction or bending moment in the cap) are sensitive to (or *loosely speaking*, depend on) the random variable $L$ while they have no sensitivity to the other random variable Ø(refer to [16] for further details). Such statement is somehow intuitively expected *a priori* as a result of using *uniform* PDF for the random variable Ø.

Referring to Fig. 4, the new center of the (*dislocated*) pile is $(X_1, Y_1)$, where

$$X_1 = L \times \cos(Ø) \quad (18)$$

$$Y_1 = L \times \sin(Ø). \quad (19)$$

In order to draw the dislocated pile with its "real circular geometry" – a key issue in the current BEM implementation/investigation – another point with coordinates $(X_2, Y_2)$ is needed on the circumference of the pile

$$X_2 = X_1 + R \quad (20)$$

$$Y_2 = Y_1 \quad (21)$$

where $R$ is the radius of the pile.

Random dislocations according to the above mentioned PDFs have been generated for four selected values of the standard deviation in the mean value of the random geometric parameter $L$ describing the position of the randomly dislocated center of the pile with respect to its original position. These four values assumed (and tried herein) for the standard deviation encompass small values of $0.1D$ and $0.2D$ up to significant deviations of $0.4D$ and $0.6D$, where $D$ is the pile diameter.

The analytical protocol as outlined above is then complemented by running the BE model thousands of time for each assumed standard deviation and for each assumed bi-axial loading condition ("ordinary" moments versus "increased" moments) using PLPAK software package (recall Sections 2 and 3 above) for randomly generated independent dislocations. Results of the overwhelming number of BE analyses are hence reported. Post-processing of the results of these Monte Carlo-BE analysis simulations has been automated in the current research. Several statistical measures have been computed for the randomly generated results including averages of piles load and bending moments in the cap, as well as dispersion estimates in these quantities using standard deviations, COV, and percentiles. Retrieved estimates for the mean values of these above mentioned design parameters as well as changes (i.e., dispersions) in such values, and the evaluation thereof, are provided in the following section.

## 5. Parametric numerical study and discussion of statistical results

The results of the extensive parametric statistical study outlined above are presented and assessed in this section. It is worth mentioning that alternative statistical measures are used to characterize the central tendency of the design parameters of interest to this research, namely: pile load and bending moment in the pile cap. Adopted measures for the central tendency include: sample arithmetic mean (or simply the *mean* as referred to in what follows), and sample counted median. The latter is basically the 50th percentile of the generated random results. The counted median may particularly have the advantage of being less sensitive to outliers (i.e., individual observations that are significantly larger or smaller than the rest of the sample) than the sample mean. A few selected results comparing the two central tendency measures investigated in the current research are first presented. However, due to space limitations, for the rest of data demonstrated in this paper the focus is only on the *mean* for simplicity without loss of generality. Furthermore, for a comprehensive statistical evaluation of the resulting random values of the design parameters of interest in this research, it is important to quantify the level of dispersion (i.e., scatter or spread) that exists around retrieved expected mean values. A common and effective way to measure such dispersion is through the COV as mentioned before, which is defined as the ratio of the standard deviation to the mean and represents a normalized (non-dimensional) measure of dispersion. Nonetheless, a key disadvantage of the COV is its sensitivity to small changes in the value of the mean, especially when this mean is scoring a rather small value [17–19]. In other words, for a specific applicable example, when mean recorded bending moments along selected strips in the cap (or, mean recorded pile reaction for a particular pile within the cap) is fairly smaller than other mean values scored along other more stressed strips (or, for other more loaded piles), the resulting associated COV may occasionally score large and unrepresentative (i.e., sometimes

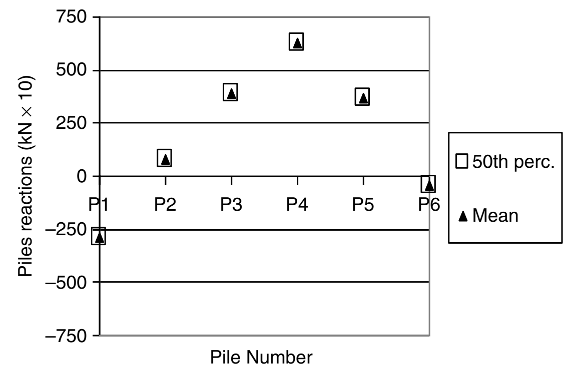


**Fig. 5.** The 50th percentile and the mean for pile reactions due to random dislocation of pile P4 with a standard deviation of $0.6D$—case of "increased" moment, 6-pile configuration.

deceiving and somehow misleading from a design-controlling perspective) values for the former less stressed strips/piles relative to the latter more stressed ones. It is worth stating that these more stressed elements intuitively carry design-controlling results. Although each and every retrieved COV associated with mean values of investigated design parameters are all theoretically and accurately determined irrespective of the level by which each element is stressed, the terms "unrepresentative" and "sometimes deceiving" are however used above. This is intended to clarify that, from a design viewpoint, reported COV values should be looked at with due care particularly in conjunction with the specific value of their corresponding means. This is in order to distinguish between design-controlling results and design-non-controlling results. Large COVs – in spite of being large – may not always control the final design if they pertain to non-controlling (*mean*) values of a given design parameter. Therefore, to be specific, concerns are mainly given to COV values corresponding to the mean bending moment at sections of maximum recorded flexure demand within the pile cap, as well as to COV values associated with the mean pile load of the most stressed pile (either in compression or in tension) within the cap.

In the context illustrated above, it has been decided to randomly dislocate the most stressed pile in compression, P4, which is a corner pile referring to the configuration of the case-study base problem shown in Fig. 1. The extreme reaction expected at this selected pile is due to the direction of applied bending moments assumed herein, the geometry of the pile cap, and the pile arrangement. Likewise, these loading and geometric characteristics of the present generic base problem lead to the most stressed pile in tension, P1, being located at the opposite corner from pile, P4, i.e., located at the other end of the diagonal of the pile cap in question (refer to Fig. 1). Moreover, for illustration purposes of the results of the current probabilistic/statistical investigation, two strips were chosen to monitor the changes in bending moment along the two main orthogonal directions of the pile cap of the case-study base problem. Both strips are located at the face of the column and near the side of the most stressed pile in compression, P4. The first strip is parallel to the pier shortest direction and the second strip is parallel to the pier longest direction (see Fig. 1). Moment $M_{xx}$ is the main moment along the first strip, while moment $M_{yy}$ is the main moment along the second strip.

Fig. 5 reveals that both measures of central tendency mentioned above (namely, the mean and the 50th percentile—or the counted median) for the resulting random pile load due to pile dislocation for the different piles within the cap of the 6-pile configuration base problem are almost exactly equal. Fig. 5 refers particularly to the more critical case of the bi-axial state of "increased" moments condition investigated herein and to the largest random dislocation considered for pile P4 (with the standard deviation of

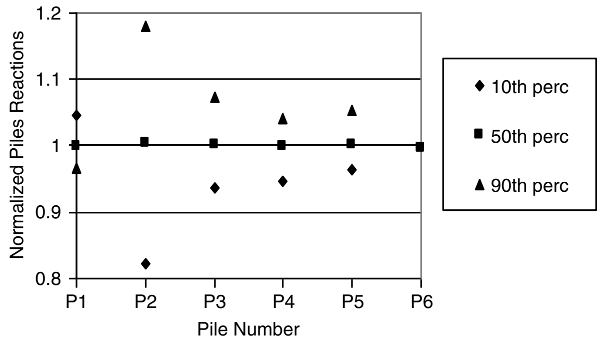


**Fig. 6.** Normalized pile reactions for different percentiles due to random dislocation of pile P4 with a standard deviation 0.6*D*—case of "increased" moment, 6-pile configuration.

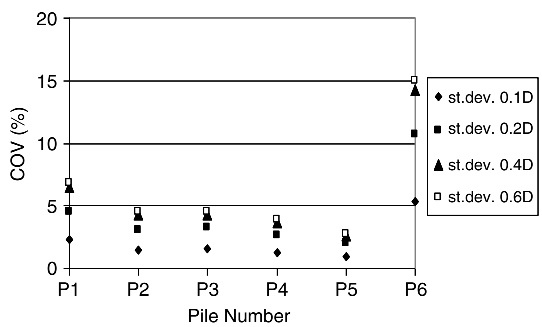


**Fig. 7a.** COV for pile reactions due to the random dislocation of pile P4 with different standard deviations—case of "ordinary" moment, 6-pile configuration.

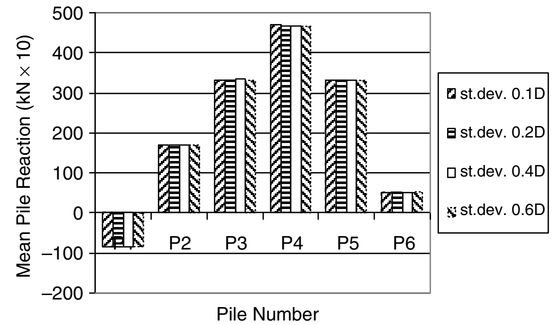


**Fig. 7b.** Mean pile reactions due to the random dislocation of pile P4 with different standard deviations—case of "ordinary" moment.

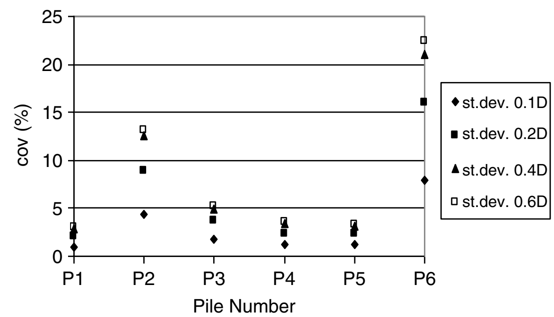


**Fig. 8a.** COV for pile reactions due to the random dislocation of pile P4 with different standard deviations—case of "increased" moment, 6-pile configuration.

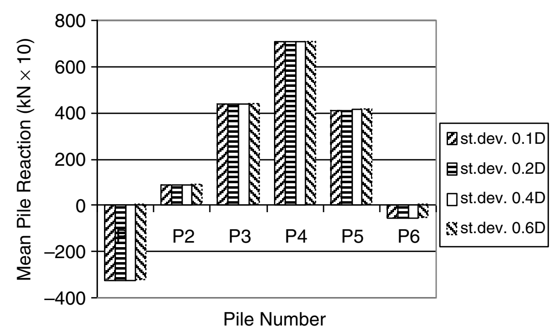


**Fig. 8b.** Mean pile reactions due to the random dislocation of pile P4 with different standard deviations—case of "increased" moment, 6-pile configuration.

the shift in the pile centroid equal to 0.6 times the pile diameter, *D*). The same trend is equally observed for bending moments along the two strips in the pile cap but is not included herein for space limitations; refer to [16] for detailed results. Such result discards any possibility of the presence of odd outliers in the retrieved random values of either the bending moments or the pile loads.

On the other hand, Fig. 6 reports the 10th, 50th and 90th percentiles for the resulting random load per different piles of the 6-pile configuration again for the "increased" moments condition and for the largest dislocation of pile P4 (corresponding to an input standard deviation in the random parameter *L* of 0.6*D*). It is obvious from the figure that the smallest dispersion in the results is scored for both the design-controlling pile in compression, P4, and the design-controlling pile in tension, P1. A much larger dispersion reflected by a significant difference in values between the 10th and 90th percentiles is however observed in the resulting random load of other non-controlling piles within the group. It is worth mentioning that a normalized pile load is given in Fig. 6 instead of the actual pile load presented in Fig. 5. The normalization is done through dividing the random (*statistical*) pile load retrieved from the dislocated case by the original (*deterministic*) pile load where no dislocation takes place.

Similar information could be also retrieved from wide-spectrum figures (such as Figs. 7a, 7b, 8a and 8b) reporting COVs in the resulting random pile load for all piles within the 6-pile configuration rectangular cap, and for the four values tried in this research for the standard deviation of the random radial shift in the center of the dislocated pile P4 (0.1, 0.2, 0.4 and 0.6 times the pile diameter). This is presented for the two sets of input bi-axial column's stress resultants: "ordinary" and "increased" moments condition, respectively. It may be generally observed that computed COVs are on the larger side for the "increased" relative to the "ordinary" moments condition. However, for the design-controlling pile in compression, P4, retrieved COV values are found almost alike for both loading conditions. COVs range from roughly a modest value of 1.5% for an input random dislocation of pile P4 with a standard deviation of 0.1*D* to a maximum value of only about 4% for a standard deviation of 0.6*D* (refer to Figs. 7a and 8a). Significantly larger dispersions reflected by COVs of about 16% and 23% for "ordinary" and "increased" moment condition, respectively, corresponding to a standard deviation of 0.6*D* for the input random pile P4 dislocation are however observed for pile P6. However, this latter pile is not carrying a design-controlling load, and hence such remarkably large reported dispersion in its load due to random dislocation of P4 is of a very minor significance to the design safety of the pile cap. For completeness, Figs. 9a and 9b provide a summary of COVs for all 6 piles within the rectangular pile cap for the two investigated cases of "ordinary" and "increased" applied moments due to random dislocation of P4 assuming a wide range of standard deviations in the random shift of the pile center (0.1, 0.2, 0.4 and 0.6*D*). Such data shall be nonetheless evaluated in the context explained above with due care in order to identify whether reported large dispersions – if any – in pile reaction control or not the design.

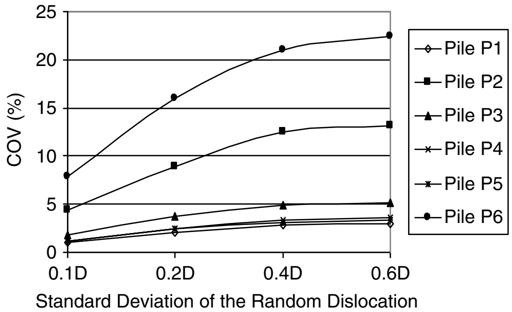


**Fig. 9a.** Effect of the standard deviation of the random dislocation on the COV for pile reactions due to the random dislocation of pile P4—case of "increased" moment, 6-pile configuration.

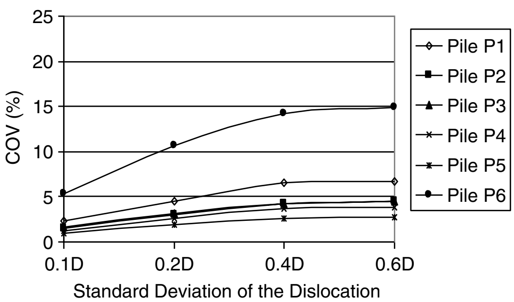


**Fig. 9b.** Effect of the standard deviation of the random dislocation on the COV for pile reactions due to the random dislocation of pile P4—case of "ordinary" moment, 6-pile configuration.

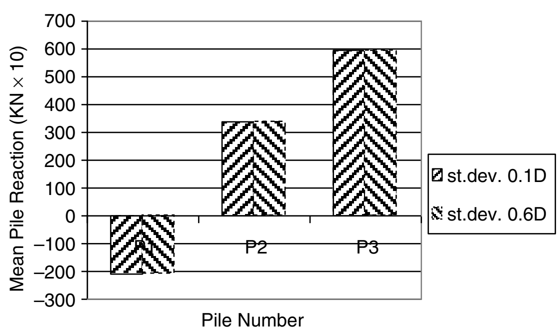


**Fig. 10a.** Mean pile reactions due to the random dislocation of pile P3 with different standard deviations—case of "ordinary" moment, 3-pile configuration.

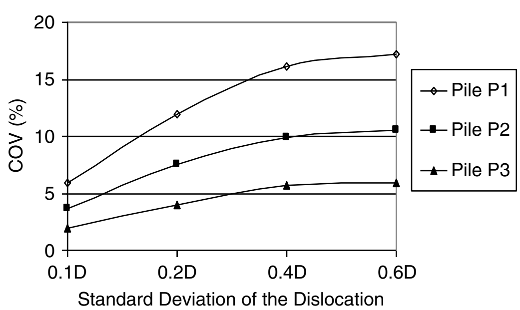


**Fig. 10b.** Effect of the standard deviation of the random dislocation on the COV for pile reactions due to the random dislocation of pile P3—case of "ordinary" moment, 3-pile configuration.

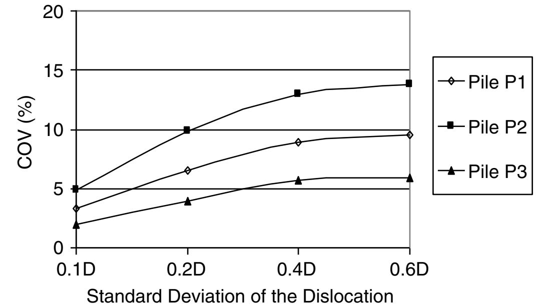


**Fig. 10c.** Effect of the standard deviation of the random dislocation on the COV for pile reactions due to the random dislocation of pile P3—case of "increased" moment, 3-pile configuration.

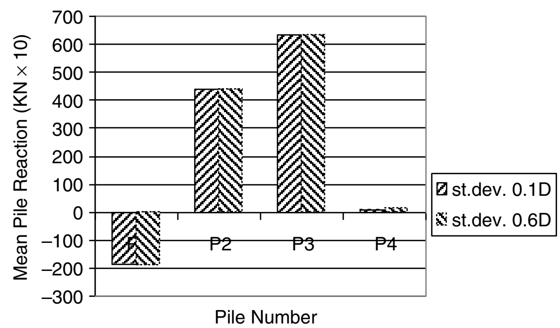


**Fig. 11a.** Mean pile reactions due to the random dislocation of pile P3 with different standard deviations—case of "ordinary" moment, 4-pile configuration.

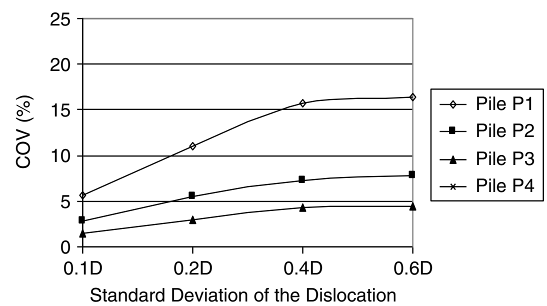


**Fig. 11b.** Effect of the standard deviation of the random dislocation on the COV for pile reactions due to the random dislocation of pile P3—case of "ordinary" moment, 4-pile configuration.

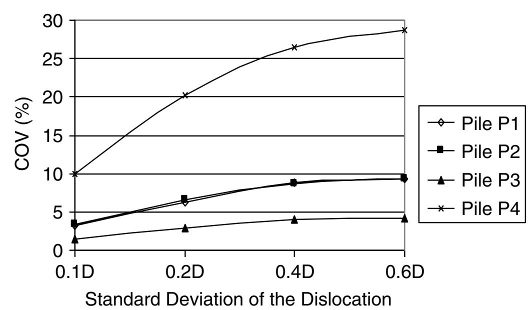


**Fig. 11c.** Effect of the standard deviation of the random dislocation on the COV for pile reactions due to the random dislocation of pile P3—case of "increased" moment, 4-pile configuration.

Figs. 10 and 11 similarly provide a summary of COVs in the resulting random loads in piles for all piles of the two additional case-study problems: namely, for the 3 piles within the 3-pile configuration with triangular pile cap and the 4 piles within the 4-pile configuration with square pile cap, respectively. Results given in Figs. 10 and 11 are for the two investigated cases of "ordinary" and "increased" applied moments due to random dislocation of pile P3 (being the most stressed pile for both the 3- and 4-pile configurations) assuming the previously introduced wide range of standard deviations in the random shift of the pile center (i.e., 0.1,

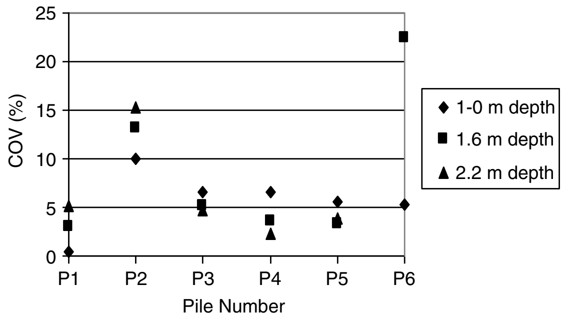


**Fig. 12.** Effect of pile cap rigidity on the COV for pile reactions due to the random dislocation of pile P4 with a standard deviation of 0.6*D*—case of "increased" moment, 6-pile configuration.

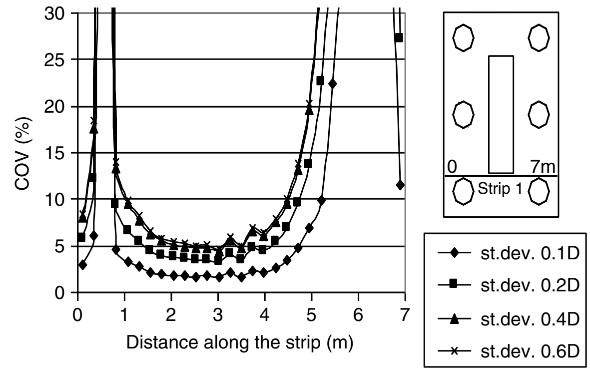


**Fig. 13a.** COV for $M_{xx}$ along the first strip due to the random dislocation of pile P4—case of "ordinary" moment.

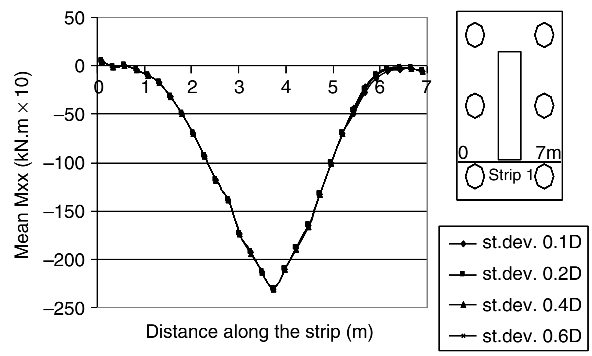


**Fig. 13b.** Mean $M_{xx}$ along the first strip due to the random dislocation of pile P4—case of "ordinary" moment.

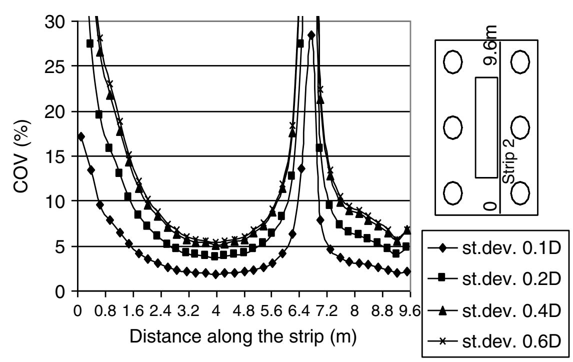


**Fig. 14a.** COV for $M_{yy}$ along the second strip due to the random dislocation of pile P4—case of "ordinary" moment.

0.2, 0.4 and 0.6*D*). Similar to observations made for the case-study base problem with the 6-pile configuration, it is noted from Figs. 10 and 11 that for the design-controlling pile in compression (P3) for the 3- and 4-pile configurations, retrieved COV values in the resulting random pile load in P3 are found almost alike for both loading conditions, i.e., "ordinary" versus "increased" moments conditions. It has been further noted that COVs in pile P3 retrieved random load range from roughly a value of 2% (for an input random dislocation of pile P3 with a standard deviation of 0.1*D*) to a maximum value of about 6% (for a standard deviation of 0.6*D*) for the 3-pile configuration (refer to Fig. 10), and from 1.5% to about 4.5% for the 4-pile configuration (refer to Fig. 11). These scored COV values in the random retrieved pile load for the design-controlling pile in compression for the 3- and 4-pile configurations are thus only very marginally larger than their corresponding values for the most stressed pile P4 in the 6-pile configuration base problem. However, it is worth mentioning that reported COVs for the most stressed pile, P3, in the 3-pile configuration score the maximum value amongst all investigated configurations as anticipated *a priori* due to the small number of piles within the group of piles affected by the dislocation.

In a further attempt to determine how much the rigidity of the pile cap may affect the variation in the pile load in case pile dislocation occurs, three pile cap depths have been tried: 1.0, 1.6 and 2.2 m, for the case-study base problem with the 6-pile configuration. It has been noted that the more the pile cap becomes rigid (i.e., a thicker cap is used), the more the COV in the most stressed piles (namely, P3, P4 and P5) reactions decreases. Furthermore, the utmost stressed pile (P4) is considered the "design-controlling" pile for the base case-study (6-pile) configuration investigated herein under the applied bi-axial bending moments as stated before, and it is therefore essential that the dispersion in the retrieved random reaction of this pile due to introduced dislocation be particularly monitored for design safety purposes. Referring to Fig. 12, for a random pile dislocation generated by an input standard deviation of 0.6*D* in the original location of pile P4, the COV in the pile P4 resulting reaction (for the case of "increased" moment condition) is around 6.5% for a pile cap depth of 1.0 m, 3.5% for a pile cap depth of 1.6 m, and finally 2.5% for a pile cap depth of 2.2 m.

Similar results are generated and presented in what follows for the mean and associated COV values of random computed bending moments $M_{xx}$ and $M_{yy}$ along pre-selected strips shown in Fig. 1 for the case-study base problem. These results are also reported for the two cases investigated herein corresponding to the two sets of applied bi-axial column's stress resultants, namely: "ordinary" moments condition, and "increased" moments condition. Information is given in form of figures showing COVs of random bending moments (describing the dispersion in the results), accompanied by other figures listing the corresponding *mean* values of these bending moments. Such illustration helps identifying the dispersion (in terms of COV) that is of importance to the flexure design of the pile cap; i.e., the dispersion associated with the *mean* "design-controlling" bending moments. Sample results are given in Figs. 13a,b–16a,b. As an example, for the case of "increased" moments investigated herein, it may be noted from Figs. 15 and 16 that COVs associated with design-controlling bending moments (either $M_{xx}$ along strip 1 or $M_{yy}$ along strip 2) score values of 2.5%, 4.5%, 6.0% and 6.5% for a random pile dislocation generated by a standard deviation of 0.1*D*, 0.2*D*, 0.4*D* and 0.6*D*, respectively, in the center of the most stressed (design-controlling) pile P4. Similar results – but with marginally lower values – could be likewise revealed from Figs. 13 and 14 for the "ordinary" moments case.

Results are also generated and presented herein for the mean and associated COV values of random computed bending moments $M_{xx}$ and $M_{yy}$ along pre-selected design strips shown in Figs. 2a

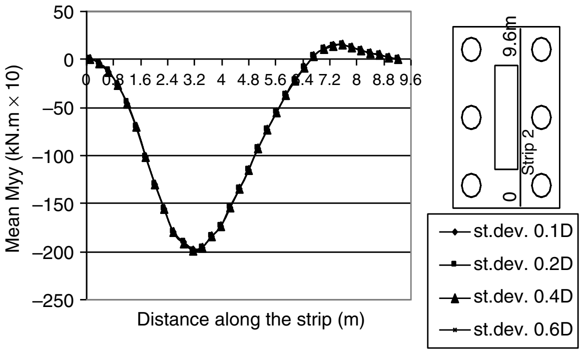


**Fig. 14b.** Mean $M_{yy}$ along the second strip due to the random dislocation of pile P4—case of "ordinary" moment.

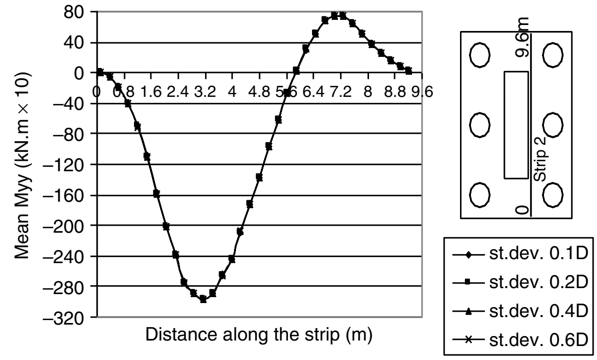


**Fig. 16b.** Mean $M_{yy}$ along the second strip due to the random dislocation of pile P4—case of "increased" moment.

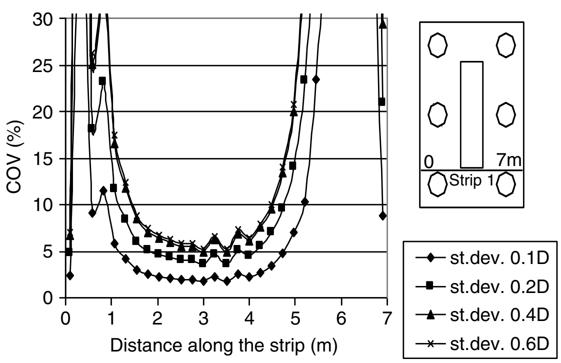


**Fig. 15a.** COV for $M_{xx}$ along the first strip due to the random dislocation of pile P4—case of "increased" moment.

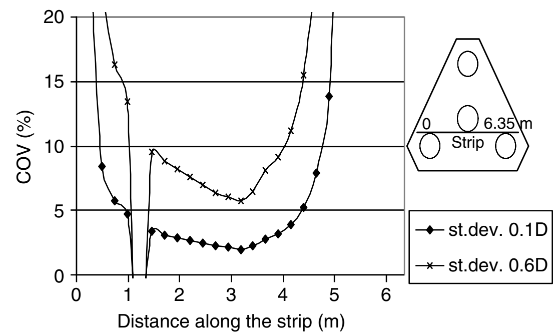


**Fig. 17a.** COV for $M_{xx}$ along the strip due to the random dislocation of pile P3—case of "ordinary" moment.

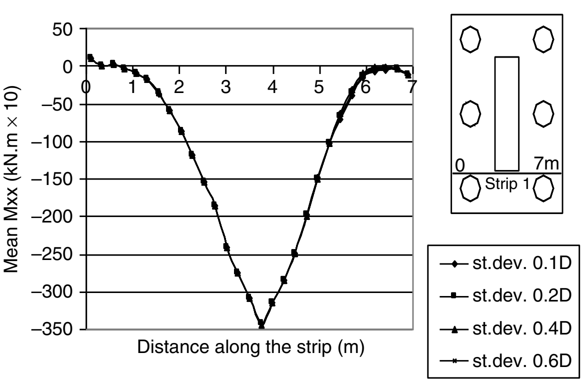


**Fig. 15b.** Mean $M_{xx}$ along the first strip due to the random dislocation of pile P4—case of "increased" moment.

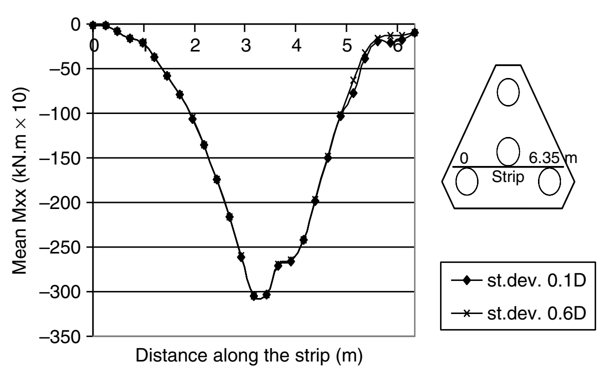


**Fig. 17b.** Mean $M_{xx}$ along the strip due to the random dislocation of pile P3—case of "ordinary" moment.

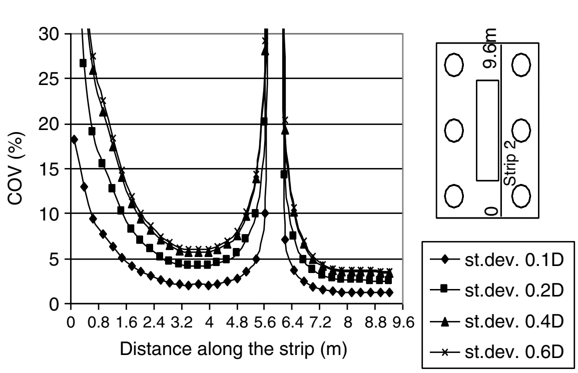


**Fig. 16a.** COV for $M_{yy}$ along the second strip due to the random dislocation of pile P4—case of "increased" moment.

and 2b for the 3- and 4-pile configuration case-study problems, respectively. These results are only reported for the "ordinary" moments condition for space limitations. It may be noted from Fig. 17 that for the triangular pile cap with the 3-pile configuration COVs associated with design-controlling bending moment ($M_{xx}$ along the critical design strip shown in Fig. 2a) score values of about 2.5% and 6.5% for a random pile dislocation generated by a standard deviation of 0.1$D$ and 0.6$D$, respectively, in the center of the most stressed pile in compression, P3. On the other hand, it may be similarly noted from Figs. 18 and 19 that for the square pile cap with the 4-pile configuration COVs associated with design-controlling bending moments (either $M_{xx}$ along strip 1 or $M_{yy}$ along strip 2 as shown in Fig. 2b) score values of about 2.5% and 6.0% for $M_{xx}$ and about 4% and 9% for $M_{yy}$ for a random pile dislocation generated by a standard deviation of 0.1$D$ and 0.6$D$, respectively, in the center of the most stressed pile in compression, P3.

Finally, conversely to the effect of increasing the cap rigidity on lessening the variation in the resulting random pile reaction

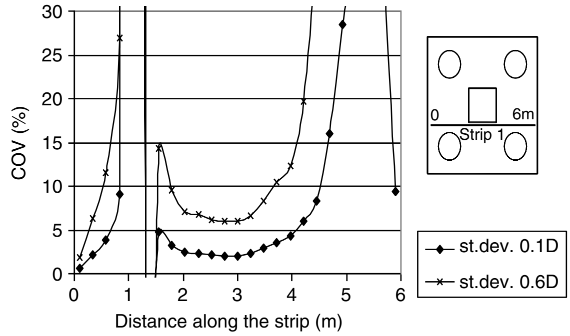


**Fig. 18a.** COV for $M_{xx}$ along the first strip due to the random dislocation of pile P3—case of "ordinary" moment.

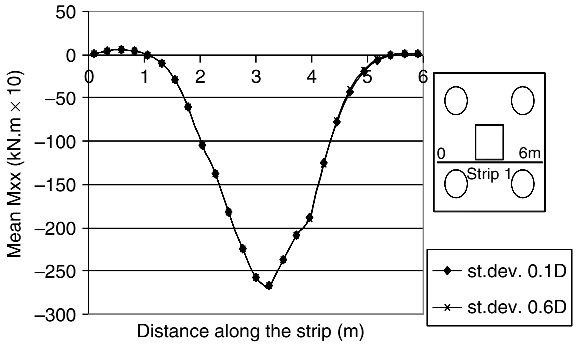


**Fig. 18b.** Mean $M_{xx}$ along the first strip due to the random dislocation of pile P3—case of "ordinary" moment.

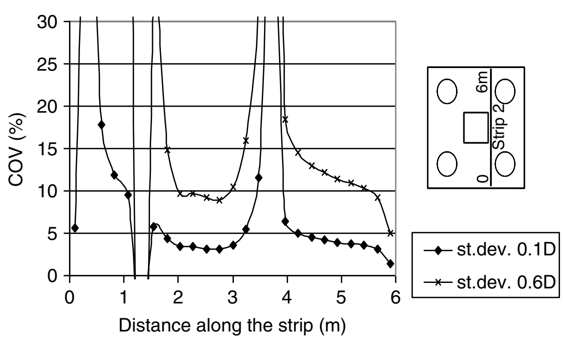


**Fig. 19a.** COV for $M_{yy}$ along the second strip due to the random dislocation of pile P3—case of "ordinary" moment.

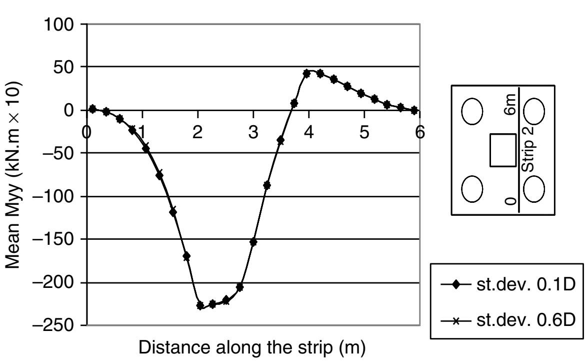


**Fig. 19b.** Mean $M_{yy}$ along the second strip due to the random dislocation of pile P3—case of "ordinary" moment.

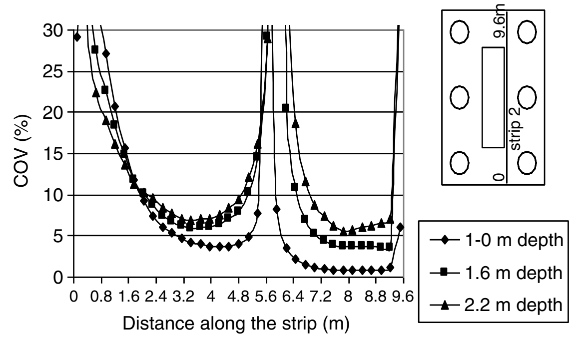


**Fig. 20a.** Effect of pile cap rigidity on the COV for $M_{yy}$ along the second strip due to the random dislocation of pile P4 with a standard deviation of 0.6*D*-case of "increased" moment.

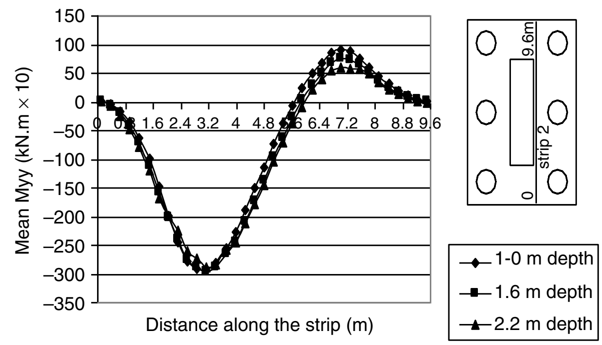


**Fig. 20b.** Effect of pile cap rigidity on the mean $M_{yy}$ along the second strip due to the random dislocation of pile P4 with a standard deviation of 0.6*D*-case of "increased" moment.

due to random pile dislocation, it has been observed that the more the pile cap becomes rigid (i.e., thicker), the more the COV in resulting bending moment values in the pile cap of the case-study base problem increases. One may refer to Fig. 20, as an example, recording the variation in the values of $M_{yy}$ along strip 2 for the case-study 6-pile configuration base problem due to random dislocation of pile P4 with a standard deviation of 0.6*D* for the "increased" moment case.

## 6. Summary and conclusions

The current research combines (a) a new BE formulation implemented to model the real circular geometry of piles supporting a polygonal pile cap, and (b) Monte Carlo simulations to model the effect of randomly shifting pile location within a given arrangement of piles (the so-called pile dislocation problems) on some selected important design parameters. The investigation is illustrated in a probabilistic/statistical context making use of the BEM that offers a powerful and efficient analysis technique for such applications. Dealing with the set of *multiple* analyses of given "pile cap–pile" systems in presence of the *random* pile dislocation problem could have been otherwise overwhelming if tackled using other analysis techniques such as FE methods. In addition to the fact that performing FE analysis for such application that encompasses thousands of successive analyses for different randomly generated dislocated positions of a particular pile is inherently time consuming, the task will further experience several meshing/re-meshing sensitivity (and accuracy) problems intrinsic to the FE method itself which adds additional modeling uncertainties (namely, *epistemic* uncertainties) to the results.

Reported results using conventional statistical measures demonstrate that the random dislocation of piles within practical ranges/values as customarily encountered for example in pile caps pertinent to bridge applications will cause limited variations in the output design parameters investigated herein, namely: pile load and bending moments in the pile cap. Other equally important design parameters such as punching shear and conventional shear demands are not covered in the present paper. To be more specific regarding presented results, it has been shown that random dislocation of a single pile (with a standard deviation up to 0.6 times the pile diameter) in a given pile cap induces a variation in the mean resultant pile reaction of the most stressed design-controlling pile, as well as in the mean value of the largest bending moments governing the flexure design of the pile cap, that is rather limited (i.e., not exceeding 9%). This value for the dispersion gets larger for other piles and bending moments at locations that are not design-controlling, and that are hence of less importance to the designer. The good news (as inferred from this reported limited dispersion in the investigated design parameters) is that the designer may then overlook a dislocated pile within a pile cap with no extra safety measures to be taken in terms, for example, of adding a substitute pile or re-checking the design safety of the affected pile cap with the dislocated piles. This is due to the fact that the dislocation is only slightly affecting the design values as demonstrated above. Furthermore, the current study ascertains that available code provisions necessitating the pile to be designed to accommodate a 10% extra load above the design load are satisfactory to ensure safety in case dislocation of a single pile occurs. The current investigation extends the usefulness of such "10% extra load" code provision – originally only addressing the pile load safety issue – to equally guarantee safe bending moments (i.e., flexure demand) in the pile caps. This is however conditioned on keeping dimensions of the affected pile cap unaltered. It has been also noted that the more the pile cap becomes rigid (i.e., its thickness increases), the more the COV in resulting pile reactions (for utmost stressed, and hence design-controlling, piles) due to random pile dislocation decreases, and the more the COV in design-controlling bending moment values increases.

The study further demonstrates that drawn conclusions presented above are valid for various investigated polygonal and symmetric pile caps (triangular, square, and rectangular) typically encountered in bridge construction practice, with number of piles up to six. Anticipated dispersion in the design parameters due to pile dislocations is expected to be further reduced for other – non-investigated – configurations of piles featuring a larger number of piles. Presented results are expected to be also equally applicable to any other applied "bi-axial bending moments–normal force" ratios rather than the two permutations investigated herein for "ordinary" and "increased" moments conditions. However, additional similar analysis effort shall be invested before blindly extrapolating current results to other general and non-symmetric "pile–pile cap" configurations that are different from those investigated herein and that are expected to be likely susceptible to overload and to anticipated important variation in the mean values of various design parameters due to random dislocation of any of their piles.

Finally, it is worth mentioning that simultaneously randomly dislocating more than one pile within a given configuration is under scrutiny by the authors in order to check whether the resulting variability in the resulting design parameters is additive or not due to these concurrently assumed dislocations when compared to individually assumed dislocations presented in the current paper. Assessing the effect of some possible correlation between such random simultaneous dislocations of several piles is also targeted.

## Acknowledgments

The authors would like to acknowledge the fruitful discussions with Dr. Ayman Awadallah of Fayoum University regarding the random simulations of the pile dislocation.

## References

[1] Moghadassi M, Cubrinovski M, Chase JG, Pampanin S, Carr A. Effects of soil-foundation-structure interaction on seismic structural response via robust Monte Carlo simulation. Eng Struct 2011;33(4):1338–47.
[2] Mehanny SSF, Ayoub AS. Variability in inelastic displacement demands: uncertainty in system parameters versus randomness in ground records. Eng Struct 2008;30(4):1002–13.
[3] Papadrakakis M, Lagaros ND, Plevris V. Design optimization of steel structures considering uncertainties. Eng Struct 2005;27(9):1408–18.
[4] Mirza SA. Monte Carlo simulation of dispersions in composite steel–concrete column strength interaction. Eng Struct 1998;20(1–2):97–104.
[5] FHWA. 1983. Allowable stresses in piles. Report no. FHWA/RD-83059. US Department of Transportation. Federal Highway Administration. Turner-Fairbank Highway Research Center Virginia. December 1983.
[6] AASHTO. 2002. Standard specifications for highway bridges. Washington (DC, USA): American Association of State Highway and Transportation Officials; 2002.
[7] International Code Council. 2009 international building code. Falls Church (VA, USA); 2009.
[8] Ambrose J. Building structures. second ed. USA: John Wiley & Sons, Inc.; 1993.
[9] Rashed YF. Boundary element modelling of flat plate floors under vertical loading. Internat J Numer Methods Engrg 2005;62:1606–35.
[10] Rashed YF. A boundary/domain element method for analysis of building raft foundations. Eng Anal Bound Elem 2005;29:859–77.
[11] MATLAB user's guide—version 6.0. MATrix LABoratory—the language of technical computing. The MathWorks, Inc.; 2000.
[12] Reissner E. On the bending of elastic plates. Quart Appl Math 1947;5:55–68.
[13] Vander WeeënF. Application of the boundary integral equation method to Reissner's plate model. Internat J Numer Methods Engrg 1982;18:1–10.
[14] O'Neil PV. Advanced engineering mathematics. 5th ed. Thomson Pub.; 2003
[15] Sap 2000—version 14.2.4. Integrated software for structural analysis and design. Computers and Structures. CSI Berkeley. 2010.
[16] Mehanny SSF. Investigation of pile dislocation problem using probabilistic approaches and the boundary element method. M.Sc. thesis. Faculty of Engineering. Cairo University. 2011.
[17] Neter J, Kutner HK, Nachtsheim CJ, Wasserman W. Applied linear statistical models. Chicago (IL, USA): Richard D. Irwin, Inc.; 1996.
[18] Benjamin J, Cornell CA. Probability, statistics, and decisions for civil engineers. NY (USA): McGraw Hill; 1970.
[19] Ang AH-S, Tang WH. Probability concepts in engineering planning and design. Basic principles, vol. 1. NY (USA): John Wiley; 1975.